

Hydrogel-Based Injectable and Printable Calcium Phosphate Cements (CPC) – Bioactive Glass (BG) Composites for Bone Tissue Engineering

Beatriz Aráoz¹, Lara Gotthelf², Rafael A Rodriguez Acosta³, Marcos Bertuola¹, and Elida B Hermida¹

¹ITECA (CONICET-ECyT-UNSAM), Argentina. ²ECyT-UNSAM, Argentina

³Instituto Tecnológico Sabato, National Atomic Energy Commission (CNEA), UNSAM, Argentina

INTRODUCTION & AIM

Paste-like bone regeneration materials have shown clinical success across numerous dental and orthopedic applications due to their ability to be molded to repair bone defects, secure implants, and subsequently harden *in situ* to provide mechanical stability. However, their clinical use in surgical procedures remains limited because of their relatively low injectability, which restricts their applicability in minimally invasive, percutaneous interventions. This study explores a hydrogel-based approach to design composite pastes with tailored rheological, mechanical, and biological properties for bone regeneration.

METHOD

Pastes were prepared by mixing of hyaluronic acid (HA), monocalcium phosphate monohydrate (MCPM), Beta-tri-calcium phosphate (b-TCP), bioactive glass (BG 45S5) and citric acid or citrate solutions. Mechanical tests were performed in compression at 1 mm/min (Instron). Flow and time sweeps acquired in a DHR3 rheometer (1 Hz and 0.5 % amplitude).

RESULTS & DISCUSSION

Paste injectability



Figure 1: A. Smooth paste injection: representative images of the injected samples. B. Stable 3D printing: example of a well-defined, high-quality printed structure.

Rheological characterization of pastes

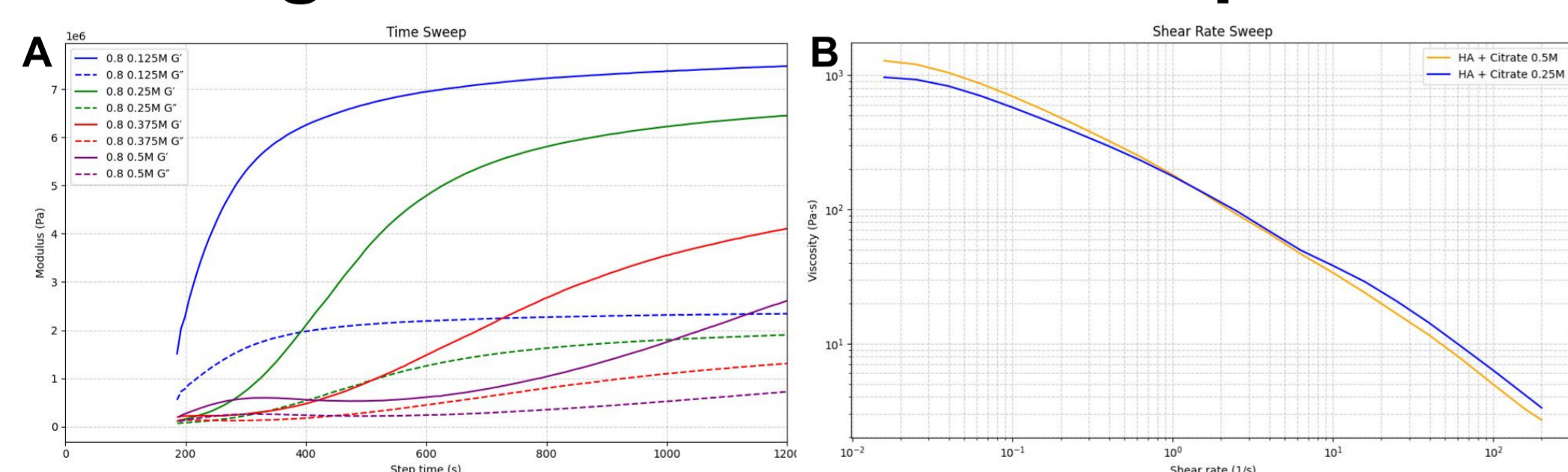


Figure 2: A. Time-sweep tests enable determination of the onset point. Increasing citrate concentration delays the onset of the reaction. B. HA in citrate solutions, 0.5 M and 0.25 M, shows shear-thinning behavior.

Setting time control

Condition	Onset	
	Rheology (s)	Optical (s)
A50	500 ± 40	1500
C4	170 ± 10	360
0.8 0.375M	484 ± 25	-
0.8 0.5M	821 ± 101	-

Table 1: influence of pH (citrate and citric acid) and L/S on setting time. Citric acid 0.5 M (A50) exhibits greater retardation than NaCitrate 0.5 M and BG (C4). A L/S ratio of 0.8 shows a longer onset time compared to 0.6 (C4).

Cement morphology

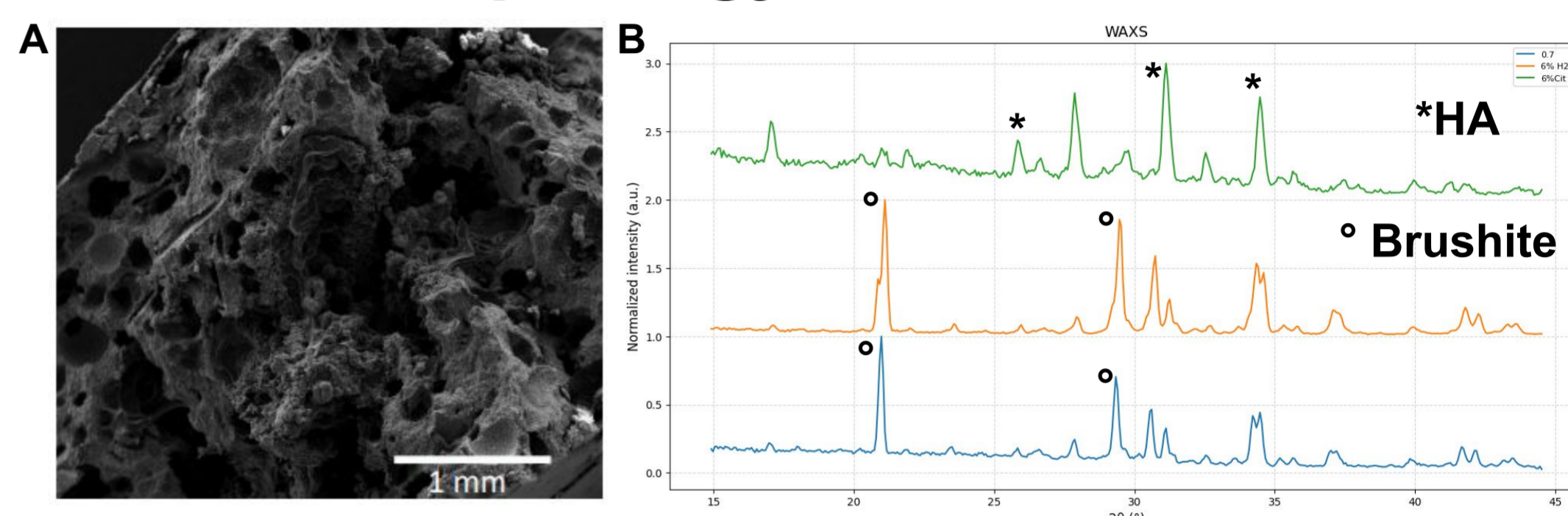


Figure 3: SEM images (A) of cements cross-sections illustrating interconnected porous structures essential for bone tissue integration, and WAXS diffractogram (B) shows pH influence on cement composition; Brushite in acidic media and hydroxyapatite in neutral media.

Mechanical characterization of cements

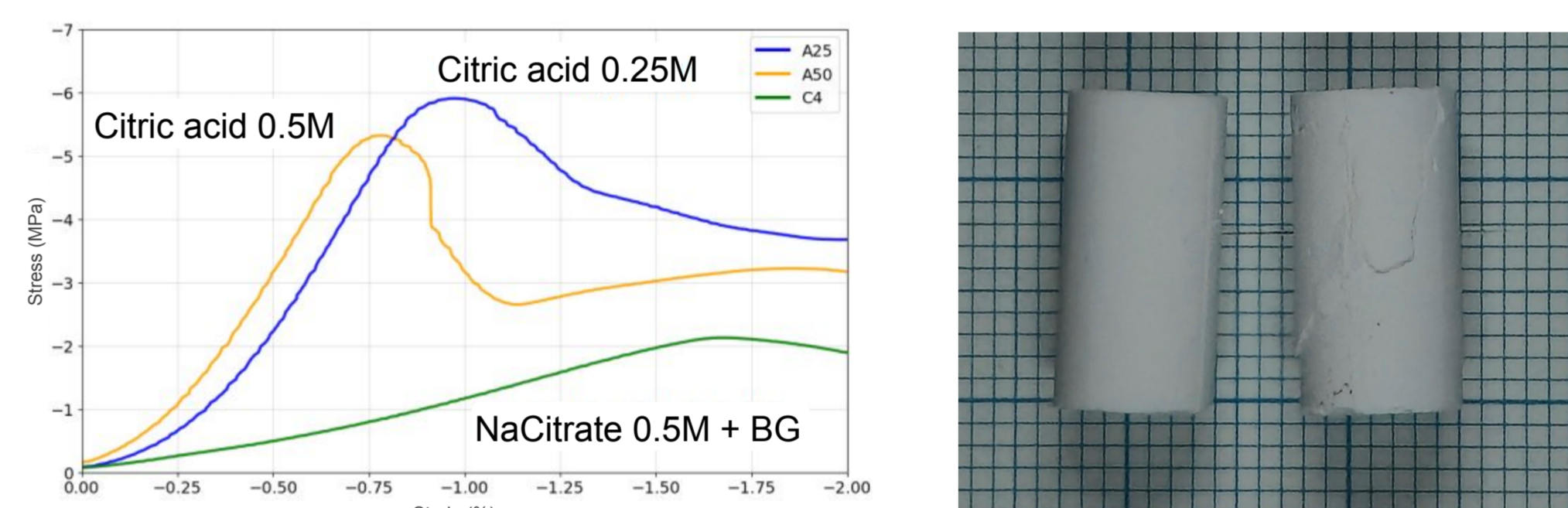


Figure 4: stress-strain curves together with images of the specimen before and after fracture. Compressive strength values between 3 and 5.5 MPa—comparable to trabecular bone—and an elastic modulus ranging from 300 to 700 MPa. The cement specimens exhibit a typical oblique failure.

Bioactivity of cements

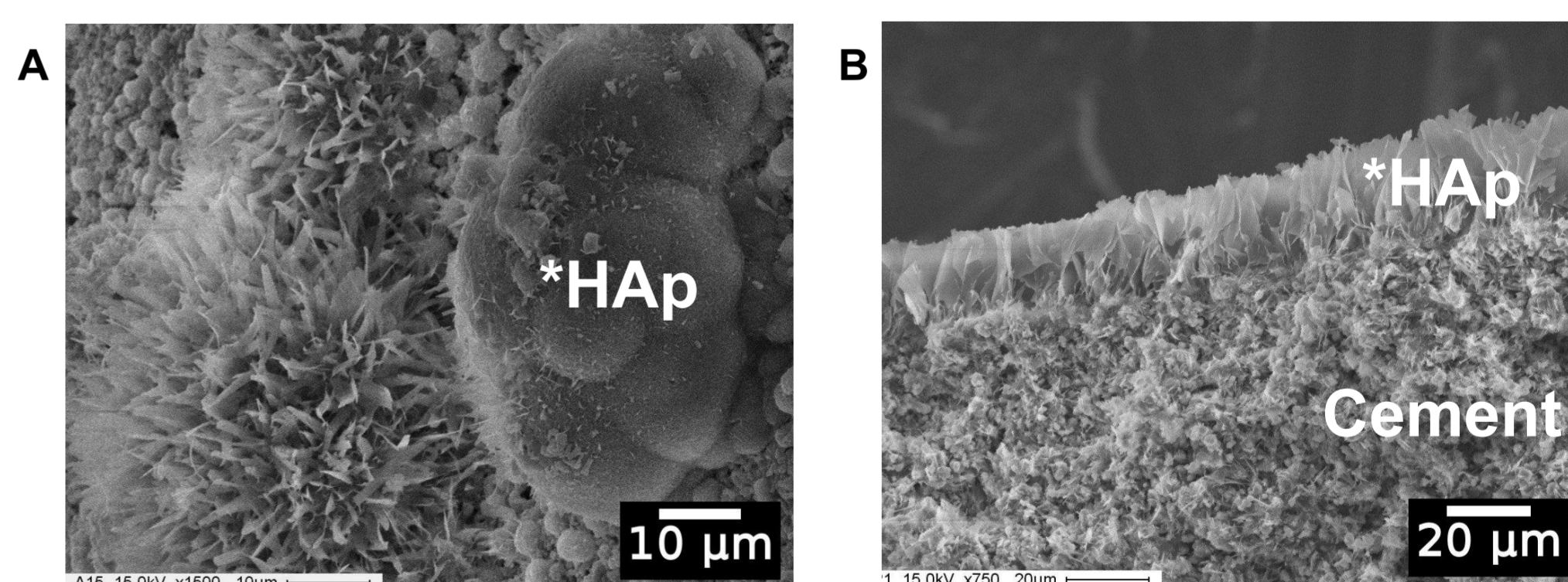


Figure 5: BG 45S5 promotes hydroxyapatite (HAP)-like layer formation in simulated body fluid at 37°C after 15 (A) and 21 (B) days of immersion, as shown by SEM surface morphology and corresponding EDS analysis (Ca/P = 1.42).

CONCLUSION

This study demonstrates the synergistic effect of hydrogels and bioactive glass in developing printable, injectable, and bioactive gel-cement composites with potential for bone tissue engineering.

FUTURE WORK / REFERENCES

Cytocompatibility tests will explore cell response towards paste and cements.

Acknowledgment: CONICET; UNSAM; Tech. Soledad Pereda, INTI. L. G gratefully acknowledges ECyT for supporting this work through a PEFI scholarship